

Fragmentation functions of charged hadrons at next-to-next-to-leading order and constraints on proton PDFs

Jun Gao^{1,2}, XiaoMin Shen^{3,1,2}, Hongxi Xing^{4,5,6}, Yuxiang Zhao^{3,6,7,8}, Bin Zhou^{1,2}

¹INPAC, Shanghai Key Laboratory for Particle Physics and Cosmology

²School of Physics and Astronomy, Shanghai Jiao Tong University, Shanghai 200240, China

³Key Laboratory for Particle Astrophysics and Cosmology (MOE), Shanghai 200240, China

⁴Institute of Modern Physics, Chinese Academy of Sciences, Lanzhou, Gansu 730000, China

⁵Key Laboratory of Atomic and Subatomic Structure and Quantum Control (MOE),

Guangdong Basic Research Center of Excellence for Structure and Fundamental Interactions of Matter, Institute of Quantum Matter, South China Normal University, Guangzhou 510006, China

⁶Guangdong-Hong Kong Joint Laboratory of Quantum Matter,

Guangdong Provincial Key Laboratory of Nuclear Science, Southern Nuclear Science Computing Center, South China Normal University, Guangzhou 510006, China

⁷Southern Center for Nuclear-Science Theory (SCNT),

Institute of Modern Physics, Chinese Academy of Sciences, Huizhou 516000, China

⁸University of Chinese Academy of Sciences, Beijing 100049, China

^{*}Key Laboratory of Quark and Lepton Physics (MOE) and Institute of Particle Physics, Central China Normal University, Wuhan 430079, China

We present the first global analysis of fragmentation functions (FFs) for light charged hadrons (π^\pm , K^\pm) at full next-to-next-to-leading order in Quantum Chromodynamics (QCD), incorporating world data from both single-inclusive electron-positron annihilation and semi-inclusive deep-inelastic scattering. The collinear factorization has been tested with low-momentum-transfer data and has demonstrated success at high hadron momenta. Additionally, we perform a joint determination of both parton distribution functions (PDFs) and FFs. Our findings indicate that the current global data on hadron production favor a reduced asymmetry in the strange (anti-) quark PDFs, as compared to the asymmetry predicted by state-of-the-art PDFs derived from inclusive data.

Introduction.– Fragmentation functions (FFs) characterize the probability density of a quark or gluon transitioning into color-neutral hadrons, expressed in terms of the light-cone momentum fraction. This concept was introduced and explained in detail by Field and Feynman in Refs. [1–3]. In addition to their fundamental role in understanding color confinement in QCD, FFs are crucial for probing the internal structure of nucleons. This becomes especially important in the upcoming precision era of high-energy nuclear physics, driven by the development of electron-ion colliders (EIC) [4, 5]. For semi-inclusive hadron production in deep-inelastic scatterings (SIDIS), a key process at the upcoming EICs, the cross sections can be factorized as hard scattering matrix elements convoluted with non-perturbative quantities, including both parton distribution functions (PDFs) and FFs [6]. State-of-the-art results for PDFs have been extracted with next-to-next-to-leading order (NNLO) accuracy in QCD through global data analyses [7–11]. In contrast, although significant efforts have been devoted to determining FFs at NNLO using data solely from single-inclusive electron-positron annihilation (SIA) [12, 13], the global analysis of FFs remains at an approximate NNLO accuracy considering both SIA and SIDIS data [14, 15].

In this letter, we present the first determination of FFs for charged pions and kaons at full NNLO accuracy in QCD, based on a global analysis of data from SIA and SIDIS. Building on advancements in theoretical precision, we are able to assess the consistency of

identified charged hadron production between e^+e^- collisions and SIDIS measurements, enabling a robust test of QCD factorization at low energy scales by incorporating recent SIA data from BESIII [16]. We find good agreements between our theoretical predictions and the data sets included in our fit, considering residual theoretical uncertainties. Furthermore, new developments have been made to enable the simultaneous determination of PDFs and FFs at NNLO accuracy in QCD for the first time. Leveraging current state-of-the-art PDFs as baselines, we achieve improved constraints on proton PDFs and uncover a preference for reduced asymmetry between strange quark and anti-quark distributions.

Theoretical setup and data characteristics.– The FFs for π^+ and K^+ are parametrized at an initial scale of $Q_0 = 1.4$ GeV using the same functional form in terms of the momentum fraction z as adopted in Refs. [17, 18]. This approach leads to a total of 53 free parameters in the analysis. The FFs are evolved to higher scales using three-loop time-like splitting kernels [19–22], implemented within a modified version of HOPPET [23], to ensure consistency with the NNLO analysis. Heavy quark FFs are non-zero but do not evolve until the mass thresholds are reached, specifically at $m_c = 1.4$ GeV and $m_b = 4.5$ GeV for charm and bottom quarks. Their contributions to low-energy SIDIS are suppressed by the heavy-quark PDFs, while those to SIA are open only at energies above the threshold for heavy meson pair production. Theoretical calculations of differential cross sec-

tions are carried out at NNLO in QCD using the FMNLO program [24, 25], which relies on perturbative coefficient functions for SIDIS calculated in [26, 27] and for SIA in [21, 28–33]. These calculations are accelerated through the use of interpolation grids and fast convolution algorithms. For calculations involving initial hadrons, the CT18 NNLO PDFs with $\alpha_S(M_Z) = 0.118$ [8] are used. We set the renormalization, factorization and fragmentation scales to be the same, with a nominal value of the momentum transfer Q for both SIA and SIDIS. Theoretical uncertainties are included in the covariance matrix of χ^2 calculations, and are assumed to be fully correlated among data sets measured at similar energies. These uncertainties are estimated by the half width of the envelope of theoretical predictions when varying all the QCD scales simultaneously by a factor of two.

We consider data sets from SIA and SIDIS with kinematic cuts of $Q > 2$ GeV and $z > 0.01$, with the hadron energy fraction defined as usual, i.e., $z \equiv 2E_h/Q$ for SIA, and $z \equiv (P \cdot P_h)/(P \cdot q)$ for SIDIS. To further test the validity of QCD collinear factorization, we impose an additional requirement on the hadron energy, setting a lower bound of $E_{h,\min}$, which will be varied during the analysis. The hadron energies are measured in the center-of-mass (Breit) frame for SIA (SIDIS). For SIA at low energies, we assume that factorization applies to the light-cone momentum fraction of the hadron, consistent with the treatment in SIDIS [2]. However, this assumption involves corrections due to the finite mass of the hadron when translating to measured distributions in terms of hadron momentum or energy [34].

For SIDIS, we utilize measurements on production of identified charged hadrons from COMPASS with isoscalar target [35, 36]. For SIA, we incorporate a comprehensive set of data from Belle, BaBar, TASSO and TPC [37–40] below the Z -pole, from OPAL, ALEPH, DELPHI, and SLD at the Z -pole [41–44], and from OPAL and DELPHI above the Z -pole [45, 46]. Importantly, we further include SIA measurements of π^\pm and K^\pm production from BESIII [16] with center-of-mass energies of 3.05, 3.5 and 3.671 GeV. These energies are much lower than the aforementioned datasets used in existing global analyses, providing a more thorough test of collinear factorization. The correlations of experimental uncertainties have been carefully accounted for, as they can significantly influence the resulting χ^2 values.

Results on FFs.— In order to test the impact of finite hadron masses and other potential power corrections on QCD collinear factorization, we perform a scan over the hadron energy cut $E_{h,\min}$ in a range of 0.5 to 1 GeV. In particular, we separate all data sets into four groups, i.e., SIA data from BESIII, B-factories, SIA data measured at high energies ($\sim 20 - 200$ GeV, HE-SIA), and SIDIS data from COMPASS. The number of data points and χ^2 for individual data set as well as global data are summarized in Table. I. An overall good agreement between

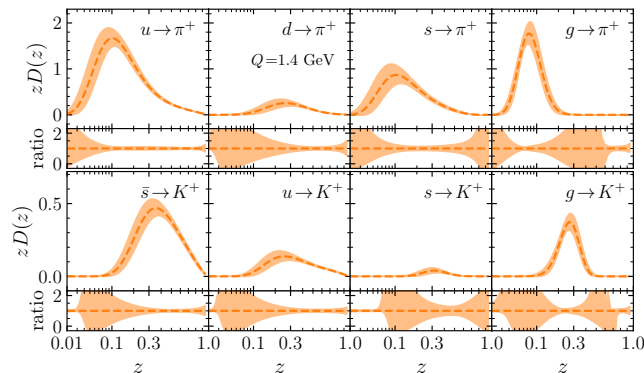
NNLO predictions of our fits and the experimental data is observed. We notice a quick growth of χ^2/N_{pt} for the global data when $E_{h,\min} < 0.8$ GeV, as well as for individual data set, especially the COMPASS data. This hints a boundary where deviations from leading twist collinear factorization begin to emerge due to finite momentum and mass effects. Consequently, we adopt a nominal choice of $E_{h,\min} = 0.8$ GeV in our following analyses, corresponding to approximately twice the mass of charged kaons. For this choice, the χ^2 of the global data is about 781.8 units for a total number of data points of 919. The agreement is good with χ^2/N_{pt} slightly below 1, and the maximum of effective Gaussian measure [8] of all data groups is 2.32σ , arising from the COMPASS data.

The extracted NNLO FFs at the initial scale for positively charged pion and kaon are shown in Fig. 1 as functions of the momentum fraction z for light quarks and gluon. We plot the Hessian uncertainty bands together with the best-fit FFs, both in absolute values and by normalized to the best-fit FFs. We use a tolerance of $\Delta\chi^2 = 2.32^2 \approx 5.4$, namely square of the maximal effective Gaussian variables of all groups, in our estimation of uncertainties of the FFs with the Hessian method [47]. We have assumed flavor symmetries at the initial scale for pion FFs from the favored quarks u and \bar{d} , pion FFs from d and \bar{u} , and pion FFs from s and \bar{s} , respectively, and for kaon FFs from all unfavored light quarks, namely s, \bar{u}, d , and \bar{d} . The pion FFs from the favored quarks are well constrained at large- z region where most of the data was measured, similarly for kaon FFs from the \bar{s} and u quarks. For $z < 0.1$, the FFs are mostly constrained by SIA data measured at or above the Z boson mass, which can probe z values as low as 0.02 after the kinematic selection. At the initial scale, the FFs from unfavored quarks are nearly negligible, except for the strange quarks fragmenting into pions. Meanwhile, the FFs from gluons exhibit a pronounced peak and are indirectly constrained through scaling violations. The FFs from heavy quarks (c and b) are also well constrained due to the heavy flavor tagged measurements in SIA. The newly published measurements from BESIII lead to strong constraints on the FFs at large- z as well as on the gluon FFs.

Importantly, developments in both theory and experiment now enable us to test QCD factorization at low Q , around a few GeV. This is achieved by examining the consistency between SIA and SIDIS data through NNLO analysis. Figs. 2 and 3 present detailed comparisons between our nominal NNLO predictions and the BESIII and COMPASS measurements of π^+ and K^+ multiplicities, shown as functions of hadron energy fraction z . All results are normalized to the central values of theoretical predictions. The error bars represent the total experimental uncertainties while the colored bands are the scale uncertainties and the Hessian uncertainties separately. The comparisons are shown for all three energies of the BESIII measurements and for various bins in Bjorken- x

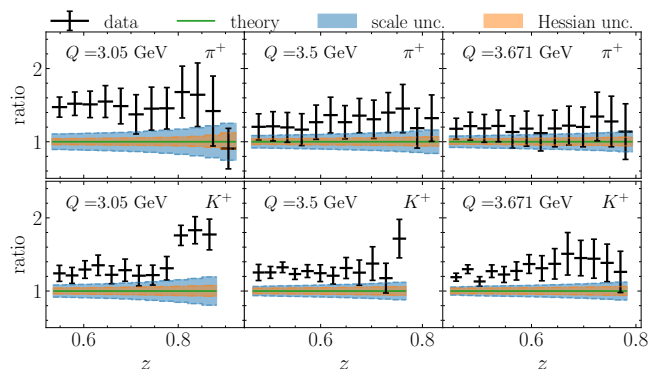
$E_{h,\min}$ [GeV]	BESIII		COMPASS		B-factories		HE-SIA		global		
	N_{pt}	χ^2/N_{pt}	N_{pt}	χ^2/N_{pt}	N_{pt}	χ^2/N_{pt}	N_{pt}	χ^2/N_{pt}	N_{pt}	χ^2	χ^2/N_{pt}
0.5	242	1.26	358	1.65	233	1.06	426	1.19	1259	1650.2	1.31
0.6	212	1.21	290	1.59	228	0.92	423	0.97	1153	1338.8	1.16
0.7	182	1.11	214	1.47	223	0.61	413	0.84	1032	997.2	0.97
0.8	152	0.98	142	1.30	218	0.53	407	0.82	919	781.8	0.85
0.9	122	1.05	94	1.29	213	0.52	407	0.80	836	687.1	0.82
1.0	98	1.14	54	0.97	209	0.49	403	0.80	764	587.2	0.77

TABLE I: Fit quality for different choices of lower cut on the hadron energy.

FIG. 1: Fragmentation functions of π^+ and K^+ for diverse partons at the starting scale $Q_0 = 1.4$ GeV. The dashed lines represent the best fit, while the uncertainties at 68% C.L. are shown in colored band.

and inelasticity y of the COMPASS measurements. The theoretical calculations are systematically below the measurements of BESIII, especially for the pion production at 3.05 GeV. However, the deficits can be largely compensated by the shifts due to both the correlated experimental uncertainties and the scale variations. On the other hand, the NNLO calculations mostly overshoot the measurements of COMPASS with scale variations to be comparable in size. Note for both the BESIII and COMPASS data the experimental uncertainties are dominated by correlated systematic uncertainties. The results are similar for π^- and K^- production. In conclusion, we find that QCD collinear factorization can simultaneously describe both SIA and SIDIS processes at Q values of a few GeV.

Constraints on proton PDFs.— We further explore complementary constraints to the state-of-the-art PDFs at NNLO, especially focusing on constraints to PDFs of the strange quarks which are less known and have been actively studied recently [48, 49]. A joint determination of FFs and PDFs by including SIDIS data can be flavor sensitive, as demonstrated in Ref. [50] with an analysis at NLO in QCD. Specifically, for the production of charged kaons in SIDIS, the differential cross sections receive large contributions from strange-quark PDFs due to the enhancement from fragmentation functions of strange quarks comparing to u and d quarks as shown in Fig. 1.

FIG. 2: Comparison of theory and data for π^+ and K^+ measurements at BESIII. The results are normalized to theoretical predictions. Q is the center-of-mass energy.

For instance, considering the difference of differential cross sections of K^+ and K^- production at COMPASS, at LO it can be expressed as

$$\frac{d^3\sigma^{K^+-K^-}}{dx dy dz} \propto 2(u_v(x) + d_v(x))(D_u^{K^+}(z) - D_{\bar{u}}^{K^+}(z)) + s_v(x)(D_s^{K^+}(z) - D_{\bar{s}}^{K^+}(z)), \quad (1)$$

where we have assumed iso-scalar target without nuclear corrections, and u_v , d_v being PDFs of valence quarks and $s_v \equiv s - \bar{s}$ being the asymmetry of strange (anti-)quark PDFs in the proton. The kinematic variables are Bjorken- x , inelasticity y and hadron energy fraction z . The COMPASS data thus are sensitive to the strange quark asymmetries in the proton giving the dominance of $D_{\bar{s}}^{K^+}$ over FFs from all other quarks, which are poorly known either from experimental measurements or from lattice calculations [51].

We select three representative values of PDFs for illustrations, which are

$$d_v \equiv d - \bar{d}, \quad r_s \equiv \frac{s + \bar{s}}{\bar{u} + \bar{d}}, \quad r_a \equiv \frac{s - \bar{s}}{s + \bar{s}}, \quad (2)$$

at a momentum fraction $x = 0.2$ and a factorization scale $Q = 2$ GeV. The central values and Hessian uncertainties are evaluated using various NNLO PDF sets, including CT18 [8], MSHT20 [9], NNPDF4.0 [10] and

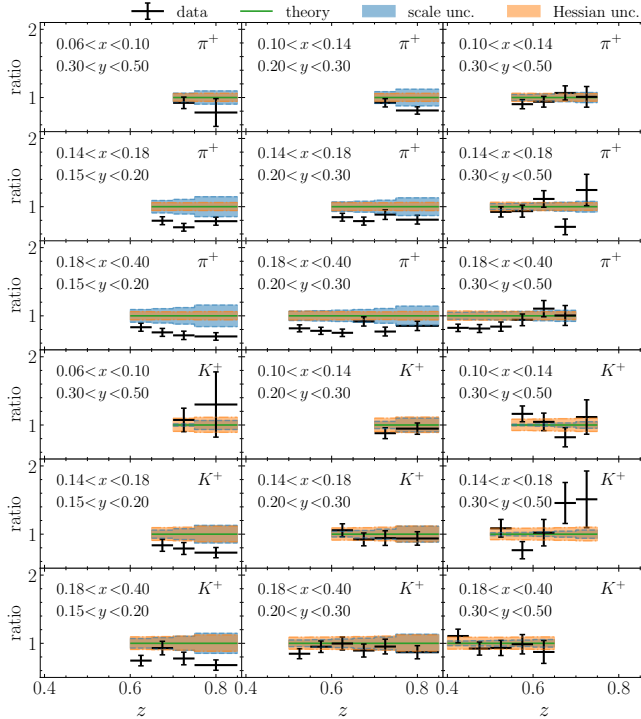


FIG. 3: Similar to Fig. 2, but for multiplicity measurements in SIDIS from the COMPASS Collaboration for different bins of Bjorken- x and inelasticity y .

ATLAS21 [11]. We repeat the prescribed fit of FFs using all above PDFs including their central PDF sets as well as error sets, and obtain the profiled χ^2 (minimized wrt. FFs) as functions of PDFs. Correlations between the profiled χ^2 and each of the PDF variables are shown in Fig. 4 with the error ellipses at 68% confidence level. Note that both the CT18 and the ATLAS21 PDFs assume $s = \bar{s}$ at the initial scale and there are only small asymmetry due to QCD evolutions [8].

We find the χ^2 exhibits strong correlations with r_s and r_a , and anti-correlations with d_v for NNPDF4.0 and MSHT20 sets. We further take them as baseline PDFs for impact study using PDF reweighting for NNPDF4.0 and PDF profiling for MSHT20 [48], respectively. In the case of NNPDF4.0 a standard Gaussian weight ($e^{-\chi^2/2}$) is used [48], while a tolerance of $\Delta\chi^2 = 10$ is used in the profiling as suggested by the MSHT20 group [9]. The results are summarized in Table. II for the three PDF values from the original PDFs and after the reweighting or profiling. The impact is more pronounced for r_s and r_a than for d_v PDFs. The NNPDF4.0 predicts a strange (anti-)quark asymmetry of more than 40% at $x = 0.2$, deviating from 0 with 3.8σ significance, while the asymmetry is 21% for MSHT20. Inclusion of the COMPASS SIDIS data reduces the asymmetry to about 28% for NNPDF4.0, and to 17% for MSHT20. The sea-quark ratio r_s is also reduced in both cases which is in agreement

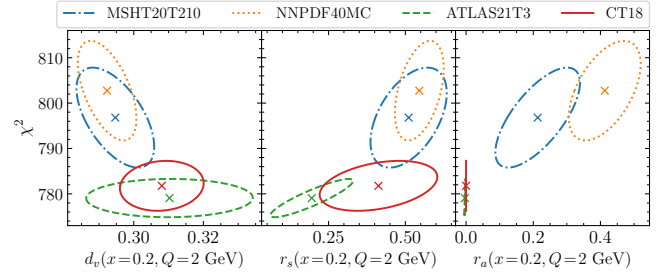


FIG. 4: Correlation between the χ^2 of fit to the hadron production data and PDF values d_v, r_s, r_a (see text for details).

with preference from data on dimuon production [52–54]. The changes of PDF uncertainties are moderate (mild) for the case of NNPDF4.0 (MSHT20).

Conclusions.– We present a comprehensive global analysis of the fragmentation functions for identified charged hadrons at full NNLO and find good agreement with hadron multiplicities measured at low- Q scales, around a few GeV, from both SIDIS and SIA processes. Our results indicate that QCD collinear factorization works well when hadrons are produced with energies greater than about twice of the hadron mass, and the FFs are well-constrained for the favored quarks. Additionally, we investigate the sensitivity of SIDIS data to proton PDFs through a joint NNLO determination of both FFs and PDFs. This analysis reveals a preference for a reduced asymmetry in the strange (anti-)quark PDFs. Our work paves the way for future studies of nucleon structure by fully exploiting the data available from electron-ion colliders.

Acknowledgments. We would like to thank M. Stolarski for communications on the COMPASS data, G. Salam for communications on the HOPPET program, and L. Harland-Lang for providing us with the alternative MSHT20 PDF sets used for profiling. The work of J.G. is supported by the National Natural Science Foundation of China (NSFC) under Grant No. 12275173 and open fund of Key Laboratory of Atomic and Subatomic Structure and Quantum Control (Ministry of Education). H. X. is supported by the NSFC under Grant No. 12475139. Y. Z. is supported by the NSFC under Grant No. U2032105 and CAS Project for Young Scientists in Basic Research Grant No. YSBR-117. X. S. is supported by the Helmholtz-OCPC Postdoctoral Exchange Program under Grant No. ZD2022004.

* Electronic address:
 jung49@sjtu.edu.cn
 xmshen137@sjtu.edu.cn
 hxing@m.scnu.edu.cn

	$d_v(x = 0.2, Q = 2\text{GeV})$	$r_s(x = 0.2, Q = 2\text{GeV})$	$r_a(x = 0.2, Q = 2\text{GeV})$
NNPDF4.0	0.2924 ± 0.0084	0.547 ± 0.079	0.408 ± 0.107
NNPDF4.0(reweighting)	0.3021 ± 0.0069	0.438 ± 0.066	0.281 ± 0.086
MSHT20	0.295 ± 0.011	0.511 ± 0.124	0.213 ± 0.126
MSHT20(profiling)	0.298 ± 0.011	0.481 ± 0.121	0.167 ± 0.136

TABLE II: PDF values d_v, r_s, r_a at 68% C.L. before and after reweighting (profiling) for NNPDF4.0 (MSHT20) PDF sets.

zb0429@sjtu.edu.cn
yxzhao@impcas.ac.cn

- [1] S. M. Berman, J. D. Bjorken, and J. B. Kogut, Phys. Rev. D **4**, 3388 (1971).
- [2] R. D. Field and R. P. Feynman, Nucl. Phys. B **136**, 1 (1978).
- [3] R. P. Feynman, R. D. Field, and G. C. Fox, Phys. Rev. D **18**, 3320 (1978).
- [4] A. Accardi et al., Eur. Phys. J. A **52**, 268 (2016), 1212.1701.
- [5] D. P. Anderle et al., Front. Phys. (Beijing) **16**, 64701 (2021), 2102.09222.
- [6] J. C. Collins, D. E. Soper, and G. F. Sterman, Adv. Ser. Direct. High Energy Phys. **5**, 1 (1989), hep-ph/0409313.
- [7] S. Alekhin, J. Blümlein, S. Moch, and R. Placakyte, Phys. Rev. D **96**, 014011 (2017), 1701.05838.
- [8] T.-J. Hou et al., Phys. Rev. D **103**, 014013 (2021), 1912.10053.
- [9] S. Bailey, T. Cridge, L. A. Harland-Lang, A. D. Martin, and R. S. Thorne, Eur. Phys. J. C **81**, 341 (2021), 2012.04684.
- [10] R. D. Ball et al. (NNPDF), Eur. Phys. J. C **82**, 428 (2022), 2109.02653.
- [11] G. Aad et al. (ATLAS), Eur. Phys. J. C **82**, 438 (2022), 2112.11266.
- [12] V. Bertone, S. Carrazza, N. P. Hartland, E. R. Nocera, and J. Rojo (NNPDF), Eur. Phys. J. C **77**, 516 (2017), 1706.07049.
- [13] M. Soleymaninia, M. Goharipour, and H. Khanpour, Phys. Rev. D **98**, 074002 (2018), 1805.04847.
- [14] I. Borsa, R. Sassot, D. de Florian, M. Stratmann, and W. Vogelsang, Phys. Rev. Lett. **129**, 012002 (2022), 2202.05060.
- [15] R. Abdul Khalek, V. Bertone, A. Khoukli, and E. R. Nocera (MAP (Multi-dimensional Analyses of Partonic distributions)), Phys. Lett. B **834**, 137456 (2022), 2204.10331.
- [16] M. Ablikim et al. (BESIII) (2025), 2502.16084.
- [17] J. Gao, C. Liu, X. Shen, H. Xing, and Y. Zhao, Phys. Rev. Lett. **132**, 261903 (2024), 2401.02781.
- [18] J. Gao, C. Liu, X. Shen, H. Xing, and Y. Zhao, Phys. Rev. D **110**, 114019 (2024), 2407.04422.
- [19] A. Mitov, S. Moch, and A. Vogt, Phys. Lett. B **638**, 61 (2006), hep-ph/0604053.
- [20] S. Moch and A. Vogt, Phys. Lett. B **659**, 290 (2008), 0709.3899.
- [21] A. A. Almasy, S. Moch, and A. Vogt, Nucl. Phys. B **854**, 133 (2012), 1107.2263.
- [22] H. Chen, T.-Z. Yang, H. X. Zhu, and Y. J. Zhu, Chin. Phys. C **45**, 043101 (2021), 2006.10534.
- [23] G. P. Salam and J. Rojo, Comput. Phys. Commun. **180**, 120 (2009), 0804.3755.
- [24] C. Liu, X. Shen, B. Zhou, and J. Gao, JHEP **09**, 108 (2023), 2305.14620.
- [25] B. Zhou and J. Gao, JHEP **02**, 003 (2025), 2407.10059.
- [26] S. Goyal, S.-O. Moch, V. Pathak, N. Rana, and V. Ravindran, Phys. Rev. Lett. **132**, 251902 (2024), 2312.17711.
- [27] L. Bonino, T. Gehrmann, and G. Stagnitto, Phys. Rev. Lett. **132**, 251901 (2024), 2401.16281.
- [28] P. J. Rijken and W. L. van Neerven, Phys. Lett. B **386**, 422 (1996), hep-ph/9604436.
- [29] P. J. Rijken and W. L. van Neerven, Phys. Lett. B **392**, 207 (1997), hep-ph/9609379.
- [30] P. J. Rijken and W. L. van Neerven, Nucl. Phys. B **487**, 233 (1997), hep-ph/9609377.
- [31] A. Mitov and S.-O. Moch, Nucl. Phys. B **751**, 18 (2006), hep-ph/0604160.
- [32] G. Soar, S. Moch, J. A. M. Vermaseren, and A. Vogt, Nucl. Phys. B **832**, 152 (2010), 0912.0369.
- [33] Z. Xu and H. X. Zhu (2024), 2411.11595.
- [34] S. M. Moosavi Nejad, M. Soleymaninia, and A. Maktoubian, Eur. Phys. J. A **52**, 316 (2016), 1512.01855.
- [35] C. Adolph et al. (COMPASS), Phys. Lett. B **764**, 1 (2017), 1604.02695.
- [36] C. Adolph et al. (COMPASS), Phys. Lett. B **767**, 133 (2017), 1608.06760.
- [37] M. Leitgab et al. (Belle), Phys. Rev. Lett. **111**, 062002 (2013), 1301.6183.
- [38] J. P. Lees et al. (BaBar), Phys. Rev. D **88**, 032011 (2013), 1306.2895.
- [39] W. Braunschweig et al. (TASSO), Z. Phys. C **42**, 189 (1989).
- [40] H. Aihara et al. (TPC/Two Gamma), Phys. Rev. Lett. **61**, 1263 (1988).
- [41] R. Akers et al. (OPAL), Z. Phys. C **63**, 181 (1994).
- [42] D. Buskulic et al. (ALEPH), Z. Phys. C **66**, 355 (1995).
- [43] P. Abreu et al. (DELPHI), Eur. Phys. J. C **5**, 585 (1998).
- [44] K. Abe et al. (SLD), Phys. Rev. D **69**, 072003 (2004), hep-ex/0310017.
- [45] G. Abbiendi et al. (OPAL), Eur. Phys. J. C **27**, 467 (2003), hep-ex/0209048.
- [46] P. Abreu et al. (DELPHI), Eur. Phys. J. C **18**, 203 (2000), [Erratum: Eur.Phys.J.C 25, 493 (2002)], hep-ex/0103031.
- [47] K. Kovařík, P. M. Nadolsky, and D. E. Soper, Rev. Mod. Phys. **92**, 045003 (2020), 1905.06957.
- [48] J. Gao, L. Harland-Lang, and J. Rojo, Phys. Rept. **742**, 1 (2018), 1709.04922.
- [49] S. Amoroso et al., Acta Phys. Polon. B **53**, 12 (2022), 2203.13923.
- [50] E. Moffat, W. Melnitchouk, T. C. Rogers, and N. Sato (Jefferson Lab Angular Momentum (JAM)), Phys. Rev. D **104**, 016015 (2021), 2101.04664.
- [51] T.-J. Hou, H.-W. Lin, M. Yan, and C. P. Yuan, Phys. Rev. D **107**, 076018 (2023), 2211.11064.
- [52] D. Liu, C. Sun, and J. Gao, JHEP **08**, 088 (2022), 2201.06586.

[53] J. Gao, JHEP **02**, 026 (2018), 1710.04258.

[54] E. L. Berger, J. Gao, C. S. Li, Z. L. Liu, and H. X. Zhu,

Phys. Rev. Lett. **116**, 212002 (2016), 1601.05430.